Modeled phytoplankton diversity and productivity in the California Current System

Ecological Modelling xxx (2012) xxx–xxx

Contents lists available at SciVerse ScienceDirect

Ecological Modelling

journal homepage: www.elsevier.com/locate/ecolmodel

Modeled phytoplankton diversity and productivity in the California Current System

N.L. Goebel[a,*], C.A. Edwards[a], J.P. Zehr[a], M.J. Follows[b], S.G. Morgan[c]

[a] Ocean Sciences Department, University of California, Santa Cruz, CA 95064, USA
[b] Department of Earth, Atmospheric and Planetary Sciences, Massachusetts Institute of Technology, Cambridge, MA 02139, USA
[c] Department of Environmental Science and Policy, Bodega Marine Laboratory, Bodega Bay, CA 94923, USA

ARTICLE INFO

Article history:
Available online xxx

Keywords:
Diversity
Shannon index
Species richness
Productivity
Phytoplankton
Model
California Current System

ABSTRACT

We explore the phytoplankton community structure and the relationship between phytoplankton diversity and productivity produced by a self-emergent ecosystem model that represents a large number of phytoplankton type and is coupled to a circulation model of the California Current System. Biomass of each modeled phytoplankton type, when averaged over the uppermost model level and for 5-years, spans 7 orders of magnitude; 13 phytoplankton types contribute to the top 99.9% of community biomass, defining modeled species richness. Instantaneously, modeled species richness ranges between 1 and 17 while the Shannon index reaches values of 2.3. Diversity versus primary productivity shows large scatter with low species richness at both high and low productivity levels and a wide range of values including the maximum at intermediate productivities. Highest productivity and low diversity is found in the nearshore upwelling region dominated by fast growing diatoms; lowest productivity and low diversity occurs in deep, light-limited regions; and intermediate productivity and high diversity characterize offshore, oligotrophic surface waters. Locally averaged diversity and productivity covary in time with the sign of correlation dependent on geographic region as representing portions of the diversity-productivity scatter.

1. Introduction

Aquatic ecosystems are characterized by remarkable phytoplankton diversity. One estimate places the number of phytoplankton species in the world ocean at approximately 4000 (Sournia et al., 1991), while counts of freshwater species exceed this by almost a factor of four (Bourrelly, 1985). In limited geographic regions, these numbers are reduced but still high. Cloern and Dufford (2005) observed approximately 500 distinct phytoplankton taxa within the San Francisco Bay estuary and Venrick (2009) documented nearly 300 phytoplankton taxa in the California Current eastern boundary upwelling system.

The general importance of biodiversity in ecology is widely discussed. Phytoplankton diversity in the ocean may influence the functioning of marine ecosystems through, for example, overall productivity, nutrient cycling, and carbon export. Yet most marine biogeochemical or ecosystem models are designed with limited potential for studying phytoplankton biodiversity. Early models included a single phytoplankter and one zooplankter, functionally representing simple predator-prey interactions (e.g., Franks et al., 1986; Fasham et al., 1990). Over the last 15 years, research groups have increased model complexity by including, among other changes, two (Kishi et al., 2007) and three (Moore et al., 2002) autotrophs. Importantly, ocean ecosystem models are now regularly coupled to spatially-explicit ocean circulation models, enabling spatially variable ecosystem response and the potential for niche differentiation among represented species. However, simple and complex ocean ecosystem models to date generally have ignored questions of biodiversity, focusing instead on many other important issues including understanding model dynamics (e.g., Edwards et al., 2000, Spitz et al., 2003), ecosystem response to circulation features (Edwards et al., 2000; Fiechter et al., 2009; He 2011), biogeochemical distributions (Moore et al., 2002) and biogeochemical fluxes (Fennel and Wilkin, 2009; Previdi et al., 2009).

Recently, Follows et al. (2007) developed an ecosystem model that greatly increased the number of competing phytoplankton compartments (to 78) to test phytoplankton community self-organization in a modeled global ocean. Although not all phytoplankton types were suitably adapted to compete effectively for resources, considerably more types were sustained at non-negligible concentrations than possible in more traditional models. Directly calculated diversity indices of temporally and zonally

* Corresponding author. Tel.: +1 831 459 5152; fax: +1 831 459 4882.
E-mail addresses: ngoebel@ucsc.edu (N.L. Goebel), cae@pmc.ucsc.edu (C.A. Edwards), jpzehr@gmail.com (J.P. Zehr), mick@ocean.mit.edu (M.J. Follows), sgmorgan@ucdavis.edu (S.G. Morgan).

0304-3800/$ – see front matter © 2012 Elsevier B.V. All rights reserved.
http://dx.doi.org/10.1016/j.ecolmodel.2012.11.008

averaged modeled phytoplankton revealed largest values in the tropics that decreased with latitude (Barton et al., 2010).

We have coupled this self-organizing ecosystem model to a physical circulation model of the California Current System. Goebel et al. (2010) describe the performance of this model in terms of spatial structure in total chlorophyll concentration, and biogeography and temporal progression of underlying functional groups. However, that work does not examine overall biodiversity or its structure. In this article, we examine output of the self-organizing ecosystem model output in the context of the extensive phytoplankton observations within the CCS. While the overall modeled diversity cannot compare to nature with a limit of 78 phytoplankton types (Goebel et al., 2010), it exceeds the diversity represented in most traditional marine ecosystem models.

In this paper, we examine how modeled diversity relates to productivity using an ecosystem model approach, and then compare modeled trends to those observed in nature. Multiple patterns have been documented and are shown schematically in Fig. 1. Such patterns include monotonic increases or decreases in diversity with productivity and maximum diversity at intermediate productivity that forms a unimodal or hump-shaped curve, often enveloping scattered data, or no relationship at all. The scarcity of observed concave-up (U-shape or inverse hump-shape) trends (e.g., Adler et al., 2011) precludes their inclusion in Fig. 1. Examples of these varied relationships can be found in meta-analyses of mostly terrestrial systems (Waide et al., 1999; Mittelbach et al., 2001) and aquatic benthic communities (Witman et al., 2008). Studies of pelagic aquatic environments have also documented unimodal-like structure, though usually with considerable scatter similar to that conceptualized in Fig. 1d (Agard et al., 1996; Li, 2002; Grover and Chrzanowski, 2004; Irigoien et al., 2004; Duarte et al., 2006; Spatharis et al., 2008). Cermeno et al. (2008) find no statistical relationship in their analysis of coastal, shelf, and open ocean environments. Recently Adler et al. (2011) argue, based on their meta-analysis of terrestrial plants that no simple relationship exists but that many factors contribute to variation in diversity. In this article, we test whether our model results conform to any of these trends in the diversity-productivity relationship using two diversity indices. Subsequently, we use the model to identify geographic regions and associated growth conditions that contribute to the differing portions of the diversity-productivity scatter. Agreement between modeled and observed macroecological patterns improves confidence in using this modelling approach to simulate nature and promotes future testing to determine the importance of representing such diversity in ecosystem models.

2. Methods

2.1. Self-assembling ecosystem model of the phytoplankton community

We investigate simulated phytoplankton diversity and how it relates to productivity using a 3-dimensional ecosystem model for the California Current System. Details of this ecosystem model have been documented previously (Goebel et al., 2010), and we provide only a brief description here.

The ecosystem model has structure similar to many NPZ-type marine ecosystem and biogeochemical models in the literature. At each model grid point, changes in concentrations of inorganic nutrients, phytoplankton, zooplankton, and dissolved and particulate organic matter are budgeted. What distinguishes this model from others is the relatively large number of phytoplankters represented. Here, we resolve 78 phytoplankton analogs. Each analog is randomly assigned parameters that determine physiological responses to light, nutrient and temperature. Parameter values are drawn from distributions constrained by observations and measurements reported throughout the literature. Our maximum growth rates and prescribed distributions of half-saturation levels avoid the initialization of a phytoplankter analog that would outcompete all others. We divide phytoplankton into functional groups based on nutrient utilization, and each functional group is further separated into a multitude of phytoplankton types, distinguished by unique combinations of temperature, light and nutrient responses. Large phytoplankton groups include diatoms, which require silica, and large non-diatoms (LND), which do not. Small phytoplankton groups include *Prochlorococcus*-like phytoplankton (PLP), which do not use nitrate, and small non-*Prochlorococcus* (SNP), which can utilize all three forms of inorganic nitrogen. Within each phytoplankton group, approximately 20 phytoplankton types are initialized. All parameters for phytoplankton losses, and heterotrophic and remineralization processes (e.g., mortality, organic matter export, phytoplankton sinking, grazing of phytoplankton, particulate sinking, nitrification) are fixed rather than randomly prescribed. Size-based differences in sinking and reduced grazer preference for diatoms exist in the model. Phosphorus, nitrogen, and silica budgets are explicit, though phytoplankton concentrations follow Redfield ratios. Biomass and productivity reported in units of carbon are converted with a molar carbon:phosphorus ratio of 106. Carbon is converted to chlorophyll for SNP, PLP, LND, and diatoms as in Goebel et al. (2010). We note that model output used in this study is quantitatively different from than that presented in Goebel et al. (2010) (using, for example, a different random number seed to generate the exact phytoplankton community), but overall results (e.g., of functional group distributions) are qualitatively similar to the previous study.

The ecosystem model is embedded within a physical circulation model that is responsible for advection and diffusion of ecosystem component concentrations. We use the Regional Ocean Modeling System (ROMS; Shchepetkin and McWilliams, 2005), and our CCS domain extends at 1/10 degree resolution from Baja, California to the Canadian border, and to 134 W longitude. A total of 42 terrain-following levels span the water column vertically. The physical circulation is forced by atmospheric fields provided by the Coupled Ocean Atmospheric Mesoscale Prediction System (COAMPS; Hodur, 1997), a high resolution regional atmospheric model, and lateral boundary conditions are obtained from a global ocean state estimate (ECCO, Estimating the Circulation and Climate of the Ocean; Wunsch et al., 2009). More extensive details of the physical circulation model and related applications are published (Broquet et al., 2009; Veneziani et al., 2009a; Veneziani et al., 2009b; Broquet et al., 2010). Model integration extends from January 1, 1999 through December 31, 2004, with the first year treated as spin-up and not included in the analysis.

2.2. Diversity calculations and analyses of biomass and productivity

We assess phytoplankton diversity with two measures: the Shannon index (SI) and a measure of richness. The ecologically-relevant, frequency-based SI is widely used in phytoplankton ecology to portray both species richness and evenness by the uncertainty of sampling such a community at random (Legendre and Legendre, 1998). SI (dimensionless) is calculated as $H = -\sum_j^n p_j \ln p_j$, where p_j is the proportion of species j to the total biomass. A less descriptive, though perhaps more intuitive, measure of diversity also calculated is simply the number of phytoplankton types that contribute to the top 99.9% of total biomass. We consider this term as synonymous with species richness (SR) when comparing model results to observations. We calculate both SI and SR similarly, within each model grid cell volume daily for

Please cite this article in press as: Goebel, N.L., et al., Modeled phytoplankton diversity and productivity in the California Current System. Ecol. Model. (2012), http://dx.doi.org/10.1016/j.ecolmodel.2012.11.008

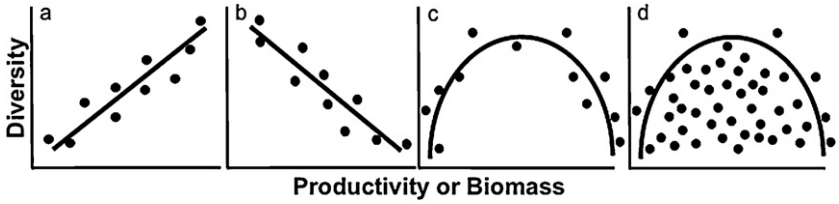

Fig. 1. Commonly observed relationships between diversity and productivity. Shown are conceptual drawings for a monotonic (a) increase and (b) decrease in diversity with productivity or biomass, and a unimodal or hump-backed trend that (c) fits or (d) envelops the data.

the full five years of the model run. It is important to emphasize that the term species diversity, as considered for both measures, is not exact for the model. Each modeled phytoplankton type does not represent a particular taxonomic species, but an entity of an unknown number of species, which includes fewer types than within a functional group. As a result, our diversity values could be considered biased low. Furthermore, we will show that many phytoplankton types contribute to the remaining 0.1% of total biomass with concentrations spanning over 4 orders of magnitude. Modeled phytoplankton types are prevented from extinction by numerically maintaining exceedingly small concentrations. These low biomass types can potentially act as seed populations though in practice, none achieves sufficient sustained growth to challenge the most competitive phytoplankton types in the top 99.9% of biomass. At locations, such as abyssal waters, where overall biomass is extremely low and phytoplankton types are numerically sustained, diversity metrics are artificially high. In order to avoid this misrepresentation, we omit from the diversity calculations phytoplankton types with biomass below a prescribed limit (1e−5 μM P).

One factor that influences diversity calculations in nature is dispersal limitation (Partel and Zobel, 2007). Physical transport mechanisms do not uniformly disperse all species throughout a region. Thus in any given zone, some species are unable to compete for resources because they have never been transported to the area and do not exist locally. In our modelling study, this factor does not apply because all phytoplankton types are initialized identically within each model cell and, as mentioned above, poorly adapted types whose concentration continues to decline are numerically sustained at vanishing but still positive levels. As a result, all phytoplankton types are available at all grid cells and all times to compete for resources and potentially contribute to calculated diversity. Therefore, while dispersal is explicitly modeled with divergences and convergences resulting in local decreases and increases in concentration, differences in the growth response, grazing factors, and the changing physical, chemical and biological environment play a larger role in shaping the diversity and biogeography of the phytoplankton community.

Members of the phytoplankton community are ranked by contribution to total biomass in the surface domain. We determine each phytoplankton type's surface biomass by integrating its biomass across all (181×186) horizontal grid cells at the uppermost grid level, normalizing by the associated volume, and averaging over all 1828 daily snapshots of the 5-year model experiment. For identification purposes, each type is assigned a unique phytoplankton number, from 1 to 78, which is arbitrary, determined by its order of initialization.

We compare diversity and productivity across three different locations of the model domain. At each location, profiles of diversity indices and productivity are averaged over 4 square degrees that consist of approximately 440 data points; a square block of points represents the south (35.9N–37.9N, 129.1W–131.1W) and north (44.0N–46.0N, 129.1W–131.1W) offshore regions, while a nearshore strip of points represents the coastal subregion that extends from the coast to the 500 m model isobath between latitudes 36.0N and 44.6N. We investigate how the model output from these daily profiles of diversity and productivity vary with time and depth. ROMS uses a terrain-following coordinate system in the vertical. Therefore, the depth of model levels varies spatially over averaged regions. At the south offshore subregion, the average depth and standard deviation is 4.2 ± 0.1 m at the surface, while the deep ROMS level spans 158 m to 170 m and averages 165 m. The surface coastal subregion tested averages 0.3 m depth, ranging from 0.14 m to 0.53 m.

3. Results

Of the 78 randomly parameterized phytoplankton types initialized in the model, 13 types contribute to the upper 99.9% on average, and up to 17 types instantaneously. The percentage of each phytoplankton type's contribution to this average biomass concentration is calculated and yields the species abundance distribution, shown in Fig. 2a as a function of phytoplankton number ordered by biomass. The steep decline in percentage with ranked phytoplankton number demonstrates that the majority of the biomass (76%) consists of a few types, namely two diatoms located primarily in coastal waters, and a small non-*Prochlorococcus* (SNP) found in both north offshore and coastal waters (Fig. 3a-c). The fourth and fifth highest types include a central to southern offshore PLP and a SNP that is found in south offshore and coastal waters (Fig. 3d-e). The other top phytoplankton types include 3 diatoms, 2 SNP, and 3 small *Prochlorococcus*-like (PLP), but no large non-diatoms (LND). The remaining 0.1% of the total biomass includes low concentration phytoplankton types that were excluded from the calculation of diversity and can best be visualized when plotted on a log-scale (Fig. 2b). In the model, average biomass varies by over 7 orders of magnitude. While some phytoplankton types vary around their mean biomass by over 5 orders of magnitude, the top 7 types vary by less than 2 orders of magnitude and dominate the community for all seasons. In the average abundance distribution, approximately half of all phytoplankton types are numerically maintained at a prescribed minimum concentration, although additional types with means above this floor transiently experience periods at this minimum level. The dominant phytoplankton community near the surface is similar to that calculated using all depths (not shown).

One useful illustration of the modeled phytoplankton community structure is the relationship between cell size and total biomass (Fig. 4), which will be compared to observations in California coastal waters (Chavez et al., 1991; Bruland et al., 2001) and other systems (Agawin et al., 2000) in section 4.1 on model-observation comparisons. Below a total biomass of 1 mg Chl m^{-3}, modeled large cells contribute to 90% or more of total biomass, and small cells make up the remainder. At higher levels of total biomass, the percent contribution of small cells decreases dramatically, reaching only 5% of total biomass at levels above about 3 mg Chl m^{-3}.

Near the surface, diversity shows cross-shore and latitudinal gradients. Fig. 5a-b present maps of the Shannon index (SI) and species richness (SR) calculated from phytoplankton biomass averaged over the upper 20 m of the water column and the 5-year

Please cite this article in press as: Goebel, N.L., et al., Modeled phytoplankton diversity and productivity in the California Current System. Ecol. Model. (2012), http://dx.doi.org/10.1016/j.ecolmodel.2012.11.008

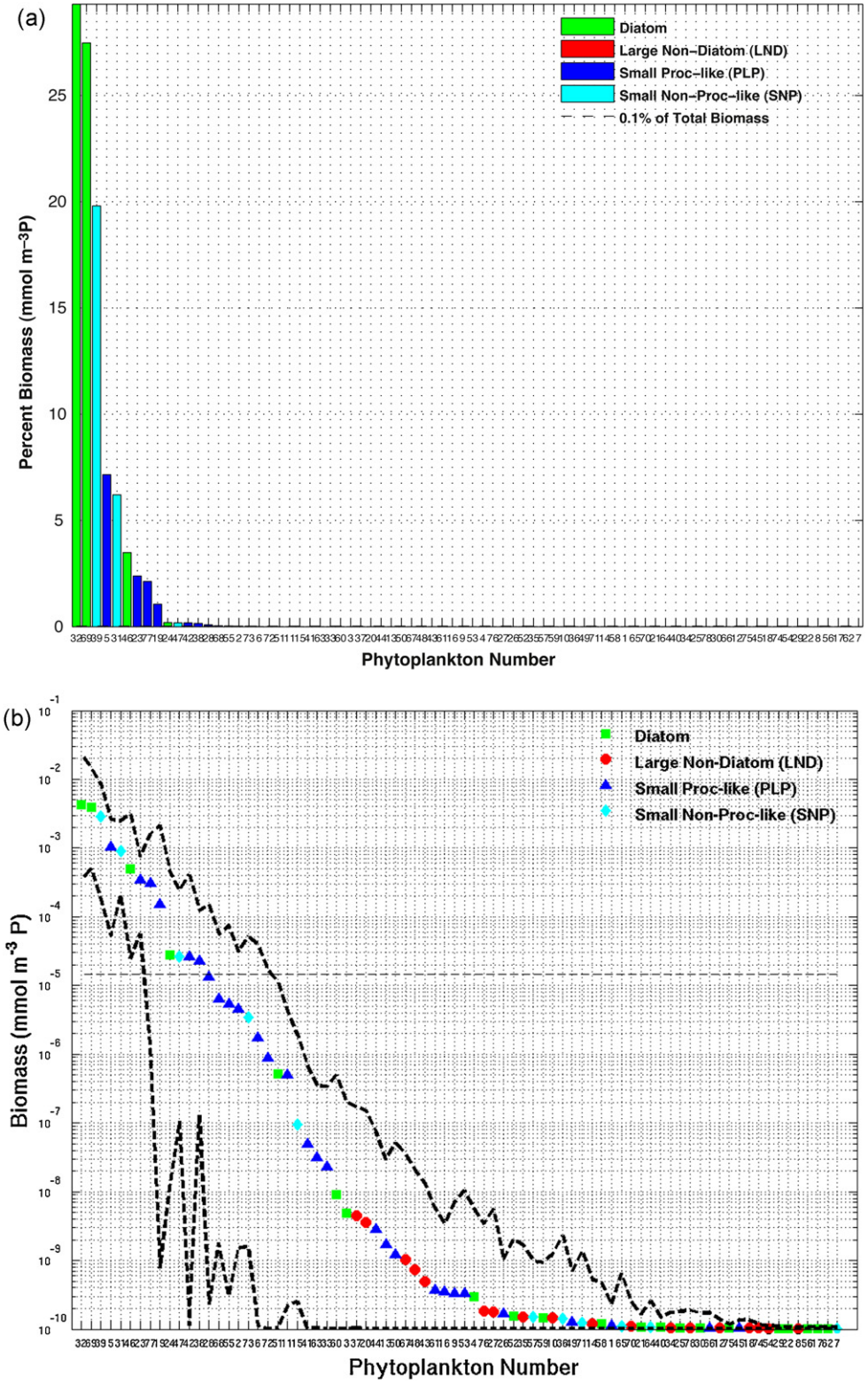

Fig. 2. Time and space averaged biomass for each phytoplankton type, ordered according to biomass and shown (a) as percent of the total averaged biomass and (b) on a logarithmic scale including maximum and minimum values attained throughout the simulation (bold dashed lines above and below mean). Phytoplankton functional groups are colored as indicated in each legend. The horizontal black dashed line indicates the level used to define species richness for this averaged plot.

duration of the model run. The domain divides into three representative regions: north offshore, coastal, and south offshore. Highest average SR (~6-8) and SI (~0.9-1.2) are found over a broad span of the region south and offshore, consisting primarily of small phytoplankton (Fig. 3d-e). In the north offshore region, the model yields lower values for both SR (~3-4) and the SI (~ = 0.4-0.6), and is dominated by a diatom and SNP (Fig. 3b-c). Generally, at all latitudes, diversity decreases as distance to the coast decreases. Within the central and northern California coastal zone, from Pt. Conception to Cape Mendocino for example, SR averages about 5

Please cite this article in press as: Goebel, N.L., et al., Modeled phytoplankton diversity and productivity in the California Current System. Ecol. Model. (2012), http://dx.doi.org/10.1016/j.ecolmodel.2012.11.008

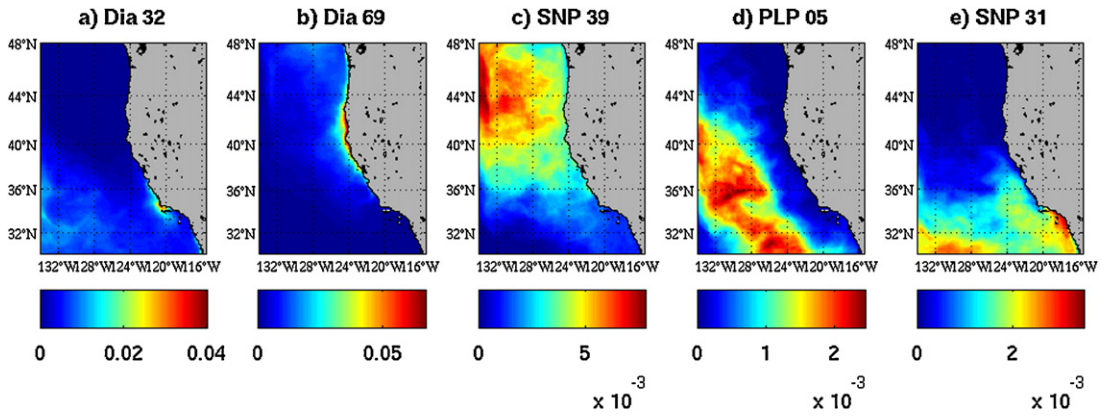

Fig. 3. Five-year average biomass (μM P) from model surface for the top 5 phytoplankton types, as shown in Fig. 2. Two diatoms (Dia), two small non-*Prochlorococcus* (SNP), and one *Prochlorococcus*-like phytoyplankter (PLP) are plotted. Note different scale bars for each plot.

while the SI averages 0.9 and includes several diatoms and SNPs (Fig. 3a-c, e).

Biological productivity near the surface, similarly averaged over the upper 20 m of the water column and over the full 5-year duration of the model run (Fig. 5c), is greatest along the central and northern California coastline, exceeding 40 mg C m^{-3} d^{-1} over a large latitudinal swath. This productivity decreases rapidly with distance offshore, up to four-fold from the coast to the coastal transition zone. Offshore, depth-integrated rates of 5-year averaged, modeled productivity varies between approximately 150-300 mg C m^{-2} d^{-1}.

A plot of productivity versus SR and SI from grid points of the model domain and daily time points of the five-year model run shows considerable scatter (Fig. 6). SR ranges from 1 to 17 with an average and standard deviation of 3.5 + - 2.6 and is discrete, taking on integer values for each space and time point; thus Fig. 6a-b presents what appear to be horizontal lines, but in fact comprise many individual points. The SI reaches values of 2.3 over a continuous range (Fig. 6c-d). To emphasize the structure of the relationship at both the low and high productivity ends of the scale, we present both logarithmic and linear versions in Figs. 6a,c and 6b,d, respectively. Both diversity indices (and their range) decrease at both low and high rates of productivity. Highest diversity is found at intermediate rates of productivity, though lower diversity also occurs at these levels. Rather than appearing as a scatter of data to which one can fit a single curve (e.g., Fig. 1c), the scatter plots suggest an upper bound for most points which fill in the area below, as shown conceptually in Fig. 1d. Depending on the diversity index used, this upper bound displays a triangular (SR) or irregular (SI) shape.

Fig. 7 presents scatter plots of productivity versus the SI at 3 locations (coastal and northern and southern offshore; see Fig. 5a and Methods for exact location of averaged area) and four depth bins for each day of the simulation. Low diversity and low productivity simultaneously occur in deep (150-200 m) waters of the south and north offshore locations while low diversity-high productivity regions are observed in the upper 20 m at the coastal location. Highest diversity is observed throughout the upper 150 m of the south offshore site in regions of intermediate rates of productivity. Variation in productivity and SI at the northern offshore location follows a similar trend to that at the southern offshore location, although with a lower peak in diversity between 50 and 150 m.

The relationship between SI and primary production varies temporally over the 5-year duration of the experiment. Fig. 8 shows time-series for both quantities from three representative regions of the domain (see Fig. 5a and Methods for exact location and averaged area). In all three cases a clear seasonal cycle in both quantities is present. In the surface waters, diversity and productivity are found to covary inversely, with peaks in production accompanying reductions in SR. This relationship is most striking in coastal waters, which is dominated by the large diatoms (Fig. 3a-b). Here, diversity rises in late summer with elevated levels extending through fall and productivity showing considerable variability but reaching elevated levels in springtime (Fig. 8a). The correlation coefficient for the near-coastal time-series is -0.69. In offshore waters at the surface, the seasonal cycle of productivity (mostly due to small phytoplankton types) is still largely out of phase with the SI, but occurs earlier in the year, generally in late winter or early spring (Fig. 8b). The correlation coefficient is -0.48, still showing a strong inverse relationship. Deeper waters offshore offer a different relationship (Fig. 8c). Diversity and productivity exhibit elevated levels during summertime, which reach minima in winter. The correlation coefficient for these time-series (0.71) is positive, in contrast to the values for surface waters. Similar trends exist for the relationship between SR and primary production (not shown).

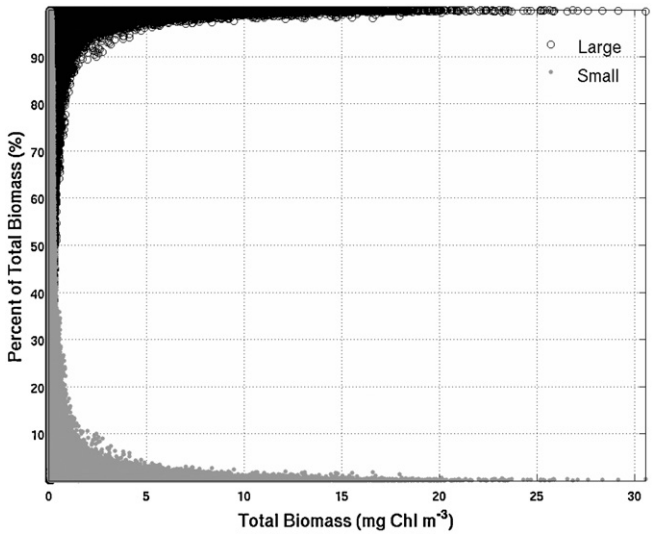

Fig. 4. Percentage contribution of small and large phytoplankton types on to the total biomass vs. chlorophyll (mg m^{-3}) concentration. Each pair of points represents one daily grid cell from the model domain. Size classes are predefined in the model by their maximum growth rate, and are not predictions of the model.

Please cite this article in press as: Goebel, N.L., et al., Modeled phytoplankton diversity and productivity in the California Current System. Ecol. Model. (2012), http://dx.doi.org/10.1016/j.ecolmodel.2012.11.008

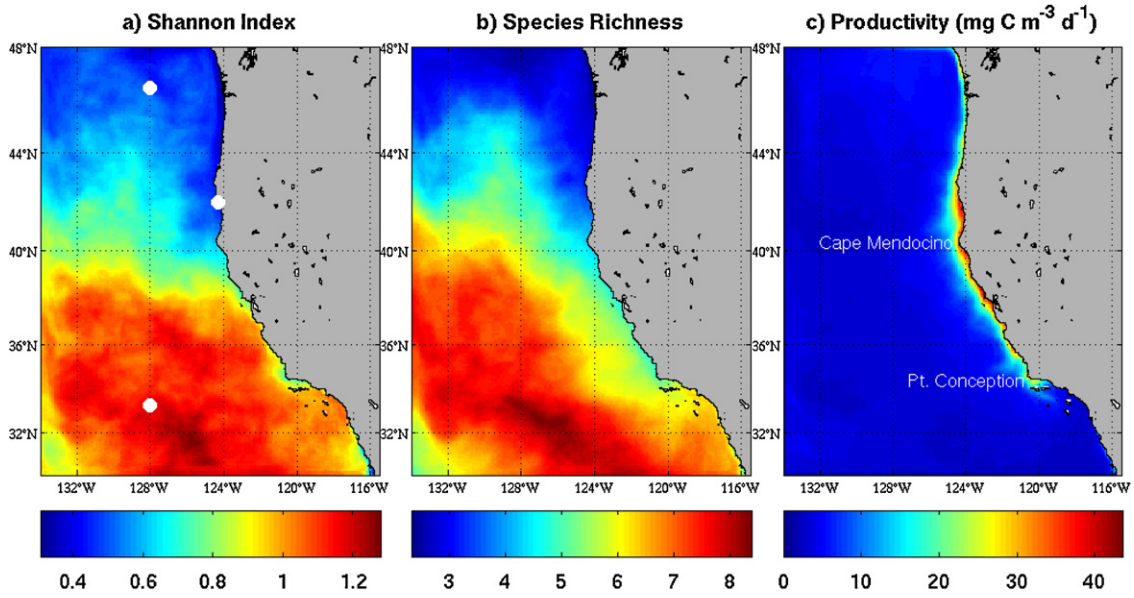

Fig. 5. Five-year averages of (a) Shannon index, (b) species richness, and (c) rates of primary production averaged over the upper 20 m of the water column (or to the ocean bottom, whichever is shallower). White circles in (a) indicate north offshore, coastal, and south offshore locations used in Fig. 7.

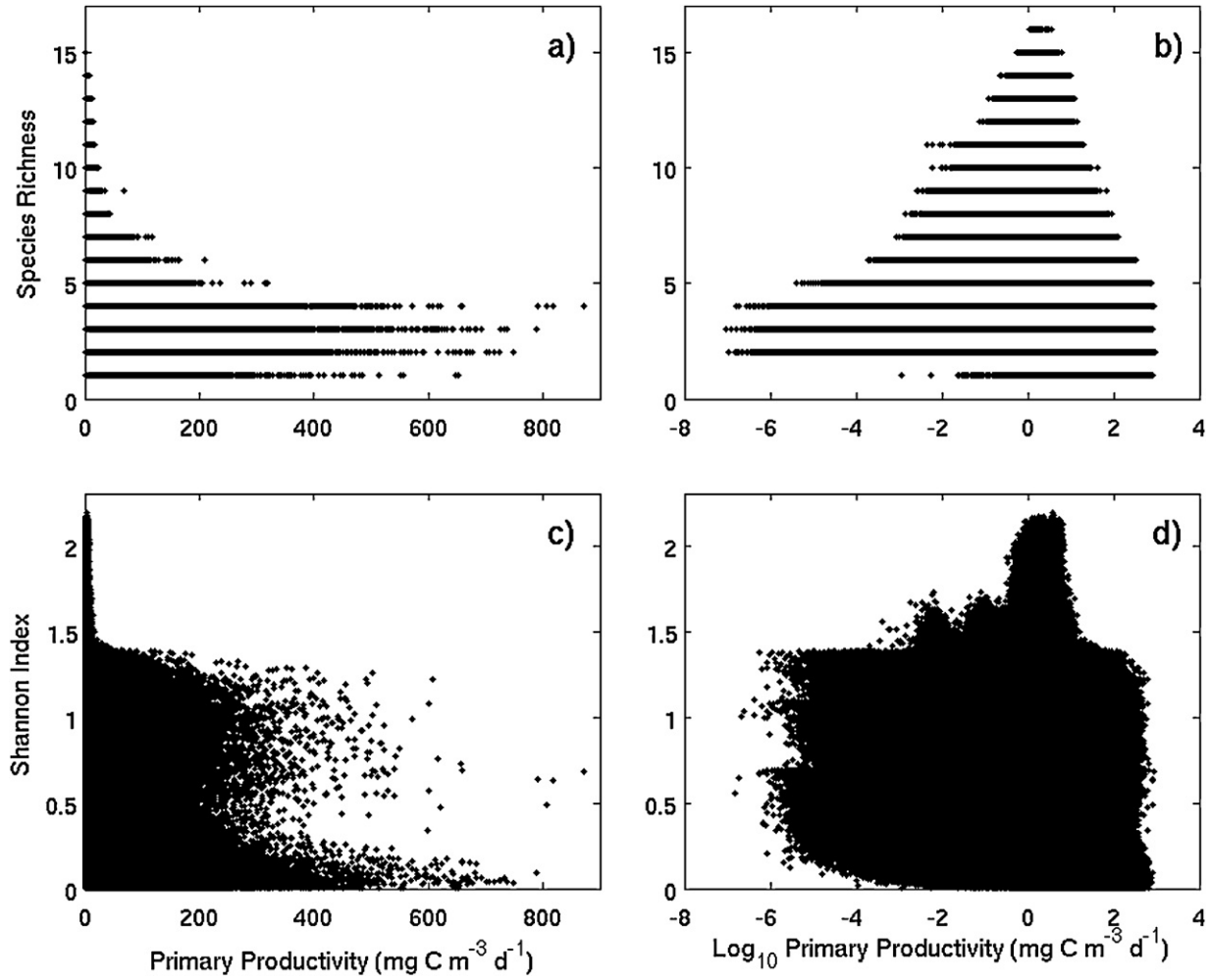

Fig. 6. Scatter plot of diversity, as species richness and Shannon index, vs. rate of primary productivity, plotted on (a, c) linear and (b, d) logarithmic scales. Each point represents one grid cell and day between 2000 through 2004 from the upper 200 m. All points where primary productivity equals zero are omitted from log scale plots. We randomly select and plot 10% of the model output.

Please cite this article in press as: Goebel, N.L., et al., Modeled phytoplankton diversity and productivity in the California Current System. Ecol. Model. (2012), http://dx.doi.org/10.1016/j.ecolmodel.2012.11.008

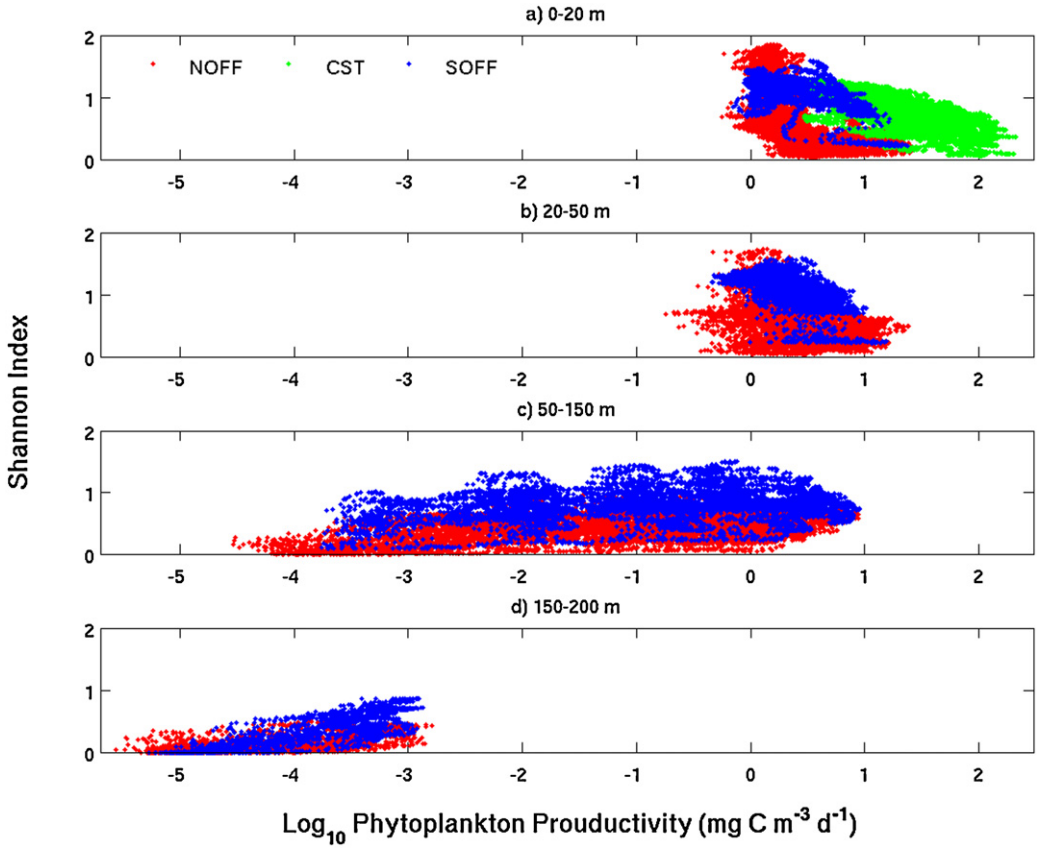

Fig. 7. Scatter plot of species richness vs. rate of primary productivity, both from one ROMS level and averaged horizontally over 4 square degrees as described in the text, at three locations shown as circles in Fig. 5: northern offshore (blue), coastal (green), southern offshore (red). Each point represents a daily value. Results are binned into four depth ranges: (a) 0-20 m, (b) 20-50 m, (c) 50-150 m, (d) 150-200 m.

4. Discussion

This modelling study analyzes emergent biodiversity within a complex community ecosystem model that resolves a large number of phytoplankton types and thus has the capability to move beyond model descriptions by size class and functional group toward investigation of planktonic species. The model setting is the California Current System. Goebel et al. (2010) evaluated overall chlorophyll structure, biogeography and seasonal variability of the functional groups and a few top phytoplankton types within this model. Here, we focus on the number of phytoplankton that contribute to the top 99.9% of total biomass (SR) and the Shannon index (SI) to evaluate diversity. In section 4.1, numbers, size, and biomass of non-negligible phytoplankton types are used to compare community structure to that observed in nature. In section 4.2, we discuss the relationship between modeled phytoplankton diversity and productivity.

4.1. Model-observation comparisons

When compared to typical ocean ecosystem models with only a few phytoplankton functional groups, the present model produces a rich phytoplankton assemblage, with average simulated SR as high as 13 and instantaneous values reaching 17. Nonetheless, this modeled diversity is still considerably less than the number of organisms documented in CCS field studies (Balech, 1960; Bolin and Abbott, 1963; Venrick, 2009) and analysis of the San Francisco bay, a CCS-influenced inlet (Cloern and Dufford, 2005). We believe this difference results from two factors. First, though the model resolves 78 phytoplankton types within 4 functional groups, each modeled type may not represent a single species, but rather a group of species. Stated differently, modeled types are parameterized to grow under overly broad environmental conditions relative to species. Our differentiation between phytoplankton types is based on parameters that vary with functional group and set requirements for light, temperature, and nutrients; alternate values of these parameters can modify modeled diversity. For example, expanding (contracting) the temperature window over which phytoplankton types thrive reduces (increases) modeled SR by reducing (increasing) the effective number of temperature niches in the system (not shown). Furthermore, species differentiation in nature is likely associated with other conditions (e.g., micronutrient requirements, light spectra) that are not included in the present model. Although we represent many important components that distinguish phytoplankton, we do not encompass the full spectrum of natural influences that characterize natural species variability. Finally, the underlying physical circulation is itself an approximation to the true oceanic motion and exists on a 1/10 degree grid. As a result, some features of the natural circulation, such as submesoscale motion, are poorly represented in the model, potentially resulting in fewer environmental niches than exist in the true California Current System.

Despite quantitative differences between absolute counts of SR in the model and observations, qualitative aspects such as the phytoplankton types that dominate and those that make up the background community compare favorably with nature. In a comprehensive study along Line 87 of the CalCOFI sampling grid in Southern California, Venrick (2009) identified 294 taxa, with 26 considered as 'dominant' using a recurrent group analysis. In their study two diatoms and one coccolithophorid accounted for 61% of

Please cite this article in press as: Goebel, N.L., et al., Modeled phytoplankton diversity and productivity in the California Current System. Ecol. Model. (2012), http://dx.doi.org/10.1016/j.ecolmodel.2012.11.008

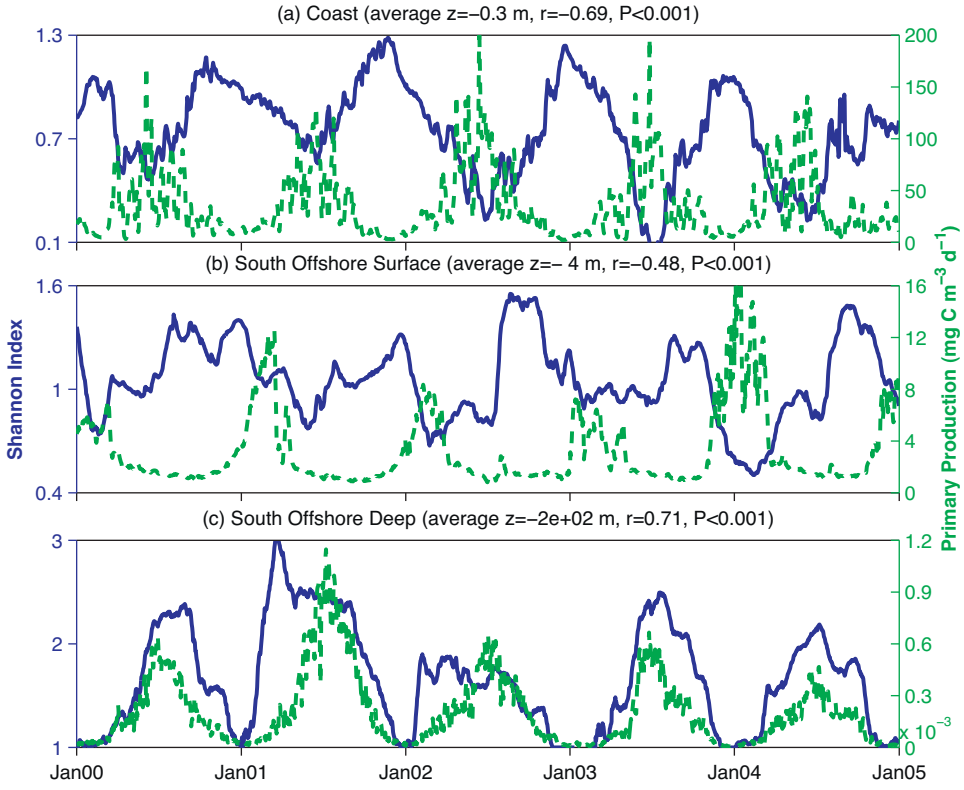

Fig. 8. Time-series of Shannon indices and rates of primary production, both from one ROMS level and averaged horizontally over 4 square degrees as described in the text. Time-series from (a) the surface level along a coastal strip, (b) the surface level from the southern offshore region, and (c) a level with average depth of 164 m from the southern offshore region. Average depth (z), and correlation coefficients between Shannon indices and productivity are displayed in plot titles.

the total biomass. Our time-averaged biomass calculations have the top three phytoplankton types (two diatoms and a SNP which potentially includes coccolithophorids) contributing to 76% of total biomass. The next 10 most dominant modeled types consist of two diatoms and two SNP and six PLP, whereas Venrick (2009) found seven diatoms, five dinoflagellates, 14 coccolithophores, one cryptomonad, and one silicoflagellate (their microscopy does not identify picophytoplankton, like *Synechococcus* or *Prochlorococcus*). In our model, the remaining 0.1% of biomass comprised 20-25 types in the time-average, themselves spanning over 4 orders of magnitude in biomass (Fig. 2b). These types arguably parallel the over 250 species counted by Venrick (2009) but not considered dominant.

Modeled cross-shore differences in diversity can also be compared to observations. Venrick (2009) identified 1 coastal and 2 offshore assemblages consisting of dominant, associated phytoplankton species along a Southern California Coast cross shore transect. The coastal assemblage consisted of five diatoms. Each offshore assemblage consisted of two to three times the number of organisms observed in the coastal assemblage and consisted of a mixed assemblage dominated by smaller phytoplankton such as coccolithophores, dinoflagellates, silicoflagellates, cryptomonads as well as diatoms. The modeled offshore community also includes a higher percentage of small phytoplankton types; analysis of the time-series shown in Fig. 8 indicates that the ratio of instantaneous SR from the southern offshore site to that at the coastal location is always greater than one, more than 1.5 over half the time, and occasionally as high as 2.8. Despite quantitative differences in diversity between model and observations, which are sensitive to parameter and formulation choice, agreement among qualitative comparisons support the likelihood that ecological mechanisms operating within the model are similar to those in nature and can provide qualitative insight into the diversity-productivity relationship.

This shift in phytoplankton size versus distance offshore can also be characterized in terms of biomass and compared to other observations. Studies have documented the dominance of small cells at low levels of total biomass (Agawin et al., 2000) and large cells in high biomass California coastal waters (Chavez et al., 1991; Bruland et al., 2001). Small cells have a superior capacity to acquire nutrients and thrive in oligotrophic waters even at low light conditions. Conversely, the higher growth rate of large cells in nutrient replete environments supports their dominance in eutrophic (e.g., coastal upwelling) systems. In addition, size specific grazing may also play a role; the rapid response of fast growing microzooplankton constrain small phytoplankton populations, whereas the slower growth of large zooplankton lags fast growing diatoms (also less palatable to grazers) leading to high diatom biomass. The modeled output produces this same division in cell size with biomass (Fig. 4). The transition at which 50% of modeled biomass comprises small cells was approximately 1 mg Chl m^{-3}, which lies in between the higher value for the CCS (Chavez et al., 1991; Bruland et al., 2001) and 0.3 mg Chl m^{-3} reported generally for open ocean and coastal waters by Agawin et al. (2000). The ability of the model to depict this structure in the phytoplankton community supports the first two principles of phytoplankton community assembly proposed by Cloern and Dufford (2005) (i.e., (1) cell size is determined by nutrient supply and selective grazing and (2) diatoms respond rapidly to nutrient pulses), and lays the foundation for an accurate representation of phytoplankton diversity in the CCS.

Modeled productivity rates compare well with nearby in situ measurements. Depth integrals of modeled productivity off Monterey Bay during summer (approximately 1200 mg C m^{-2} d^{-1}) are consistent with average measurements by Chavez et al. (1991) at the mouth of Monterey Bay in June and July of 1998 (1240 and 740 mg C m^{-2} d^{-1}, respectively). The four-fold decrease in productivity from coastal to the coastal transition zone reported by Chavez

et al. (1991) is also roughly consistent with model output. Offshore, depth-integrated rates of 5-year averaged, modeled productivity (150 - 300 mg C m^{-2} d^{-1}) is similar to satellite-based estimates of 300 mg C m^{-2} d^{-1} in the eastern portion of the North Pacific subtropical gyre (Longhurst et al., 1995). Agreement of our modeled rates of productivity with measured promotes investigation of the modeled diversity-productivity relationship.

Overall, these comparisons between observations and model output support the modeled phytoplankton assemblage as reasonable in terms of type, cell size distribution, and biogeography. With this foundation established, we discuss relationships between modeled phytoplankton productivity and diversity.

4.2. The diversity-productivity scatter

This study is motivated by the widely discussed diversity-productivity relationship as estimated in observational studies. The ocean ecosystem model used here is one of the few modelling approaches that can provide similar information from a different perspective. In our model output, SR varies between 1 and 17 and SI is as high as 2.3 across 11 orders of magnitude in productivity, both with substantial scatter (Fig. 6). This structure is differentiated by regions of the CCS that represent different ecological niches, including highly productive coastal upwelling zones, oligotrophic offshore surface waters, and deeper, low productivity habitats (Fig. 7). The upper boundary of scatter in Fig. 6 suggests a triangular (SR) or irregular (SI) shape; the lower bound argues for a flat relationship. Qualitatively, this scatter of points fill in areas whose shapes resemble that formed by the distribution of points obtained in the comprehensive studies of marine phytoplankton by Li (2002) and Irigoien et al. (2004) (Fig. 9). The range in modeled SI compares to that reported by Irigoien et al. (2004) but not to the high cytometric diversity values of Li (2002), which upon conversion of the exponential form reach high diversity values of 4.3 due to the representation of both physiological and genetic variation among organisms rather than solely taxonomy. Similar to the observed scatter reported by most observations in non-marine (Adler et al., 2011) and marine (Li, 2002; Irigoien et al., 2004; Duarte et al., 2006) systems, the scatter in our model results does not reveal a straightforward curvilinear relationship between diversity and productivity, consistent with Adler et al.'s (2011) argument that many factors contribute to the variation in diversity and therefore diversity-productivity relationships.

We tested the relationship of modeled productivity using two measures of diversity, each of which contains different information and varied shapes in their scatter of data, but resemble the scatter in the relationship. SI encompasses a balance between richness and evenness of the phytoplankton community (Li, 2002). Both SR and SI peak at intermediate values of the productivity gradient. At low productivity, phytoplankton communities have low richness and high evenness, as found in resource-deficient, deep waters represented by the left hand side of the scatter in Fig. 7d. An increase in richness results in an increase in productivity regardless of evenness. This is likely due to increased availability of resources and therefore niches that are utilized by a greater number of phytoplankton types, resulting in a more productive system. Evenness of the community further exaggerates the increase in SI with richness. At levels of productivity beyond 10 mg C m^{-3} d^{-1}, both diversity indices decrease; a lower SR will always result in lower diversity (Fig. 1a, b), and this decrease may be exaggerated by a reduction in evenness as select phytoplankton types dominate. This reduction in richness and evenness within increase in productivity is represented by the diatom-governed productive coastal waters that form the scatter on the right hand side of Fig. 7a. The interplay of evenness and richness for SI is likely responsible for distorting the shape of the scattered points (Fig. 6c-d) from that when using

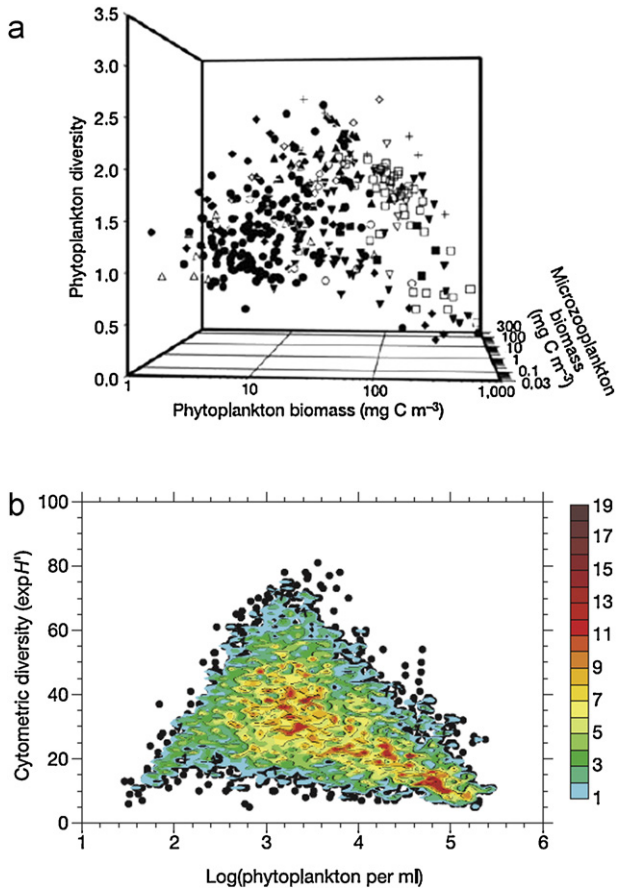

Fig. 9. Fig. 1a (a) from Irigoien et al. (2004) and (1b) (b) from Li (2002) showing observed relationships between phytoplankton diversity and biomass or abundance.

a simpler measure of diversity (SR; Fig. 6a-b). Stochasticity also plays an important role in the variability of diversity-productivity relationship scatter for models and observations (Spatharis et al., 2010).

Despite variability in the diversity-productivity relationship scatter, different regions of the modeled scatter can be interpreted through growth conditions that vary with environmental characteristics found in different regions of the model domain (Fig. 7). In the low diversity-low productivity deep offshore regions that support communities on the left side of the distribution (Fig. 7c,d), light limits phytoplankton growth (not shown). Similarly in nature, resource limitation has been shown to decrease survival and therefore phytoplankton community diversity (Hardin, 1960; Sommer, 1985; Huston, 1999; Li, 2002). High productivity and low diversity characterize coastal surface waters where growth rates of the few phytoplankton types that dominate this region exceed those of the rest of the community by at least one order of magnitude (not shown). Fast growing phytoplankton types that are optimized to outcompete the bulk of the community in typically high nutrient waters are also observed in nature (Huston, 1979; Rosenzweig and Abramsky, 1993; Huston and Deangelis, 1994).

Modeled diversity is greatest in southern offshore surface waters. Nutrient supply in this region is small relative to nearshore upwelling, but light availability is high. Thus overall resource supply could be considered intermediate as the product of both nutrient and light limitation functions determines overall growth. We find that these regions exhibit multiple phytoplankton types with similar growth rates, distinguishing them from coastal and deeper waters (not shown). Various authors have suggested reasons for the highest diversity at intermediate productivity. In a

Please cite this article in press as: Goebel, N.L., et al., Modeled phytoplankton diversity and productivity in the California Current System. Ecol. Model. (2012), http://dx.doi.org/10.1016/j.ecolmodel.2012.11.008

terrestrial study, Grime (1973) proposed high diversity occurs between extremes environmental stress. In a marine phytoplankton study from the northwestern North Atlantic, Li (2002) suggested that intermediate turbulence levels supply intermediate nutrient concentrations to the euphotic zone and enabling greater cell size diversity. In our view at intermediate resource supply, a greater number of phytoplankton types, each with different resource requirements, share similar (but suboptimal) growth rates, promoting diversity. This mechanism for coexistence in which multiple species' fitness for a particular habitat is similar, was referred to as *equalizing* in the review by Chesson (2000), which accounts for the high evenness and richness of the SI at intermediate rates of productivity discussed previously.

Temporal variability in environmental factors is also known to play an important role in shaping phytoplankton diversity and its relationship to productivity, particularly in systems lacking spatial heterogeneity (see Hutchinson, 1961; Armstrong and McGehee, 1980; Passarge et al., 2006). Temporal changes in resource supply prevent the system from reaching steady-state, causing biomass distributions to fluctuate and enhancing average diversity. Using the same self-organizing ecosystem model as the present study but in a global configuration, Barton et al. (2010) associated modeled latitudinal changes in multi-annual average diversity with seasonal variability in environmental conditions related to the time-scale for competitive exclusion. In our study of the CCS, seasonal and interannual variability in resource supply and biomass occurs in all regions, though with different amplitudes (e.g., highest amplitude associated with nearshore upwelling). As in Barton et al. (2010) we find that lower diversity accompanies greater amplitude variability. Importantly, growth and grazing rates that control phytoplankton populations and thus diversity are fast relative to seasons and enable modeled phytoplankton communities to also track longer time-scale changes in forcing. It is clear from our results that diversity and productivity are not coupled on all time-scales, further contributing to the scatter of the diversity-productivity relationship. Indeed, diversity itself results from the time-integral of growth and loss processes. This fact is visible in Fig. 8a, where high frequency variability in wind stress during spring and summer results in substantial productivity fluctuations on short time-scales, but variability in diversity during these periods is substantially muted. Finally, we have shown how the phase of correlation between diversity and productivity depends on the productivity amplitude, contributing to different portions of the overall scatter. Highly productive zones yield inverse relationships whereas low-productive regions result in positively correlated fields (Fig. 8).

It is fair to ask whether the self-organizing, multi-phytoplankton component model used here indeed benefits marine ecological studies over more traditional models with only one or two phytoplankton functional groups and considerably less computational cost. Simpler models have shown reasonable distributions of overall chlorophyll levels (Gruber et al., 2006; Omta et al., 2009) and decorrelation statistics of physical and biological fields (Powell et al., 2006). As Goebel et al. (2010) note, this self-assembling ecosystem model enables a study of biogeography that is not possible with a more traditional model. Similarly, questions of marine biodiversity can only be considered with a model that resolves a complex plankton assemblage. The model used here satisfies this requirement and exhibits reasonable chlorophyll structure, primary productivity, and relative distributions of large and small organisms for the California Current System. The modeled diversity/productivity results complement many observational studies on this subject, not supporting tight, monotonic trends but rather a loose cluster partially outlined by a hump-shaped curve. The wide range of productivities spanned by the model domain resolves a spectrum of biodiversity and reveals different temporal phase relationships between the two variables in distinct productivity zones. As marine ecosystem models become increasingly more complex, it will be interesting to see if the modeled relationship found here is robust and supported by additional investigations, or if it sensitively depends on chosen model constructs. In addition, future modelling efforts using multi-phytoplankton component models such as this one could address other marine biodiversity-related issues such as succession and complementarity effects including niche differentiation and facilitation.

Furthermore, while the general shape of the diversity-productivity scatter is likely quite robust, it is possible to speculate on how changing environmental conditions might alter ecosystem productivity and community structure. Some climate change scenarios, for example, argue for increased nutrient flux to the coastal ocean due to increased equatorial wind stress resulting from a larger land/ocean surface temperature gradient (Bakun, 1990; Auad et al., 2006). In an alternate scenario (Di Lorenzo et al., 2005), increased ocean surface temperature yields higher upper ocean stratification, a deeper thermocline, and lower vertical nutrient flux. These changes impact the high productivity, low diversity portion of our scatter plot. In the first scenario, higher nutrient fluxes should drive higher coastal productivity but still maintain low diversity, expanding the area containing the scatter. Dominance of diatoms is likely to remain unchanged in this exaggerated case of present day conditions. In the lower nutrient flux scenario, coastal productivity should be reduced (McGowan et al., 2003; King et al., 2011), possibly with some increase in diversity depending on the magnitude of nutrient flux reduction. In this case, stronger stratification of the water column and warmer temperatures may promote the presence of a higher proportion of dinoflagellate-like types in the phytoplankton community (Edwards and Richardson, 2004). Though speculative, these predictions could be tested through analysis of this model in climate change conditions, which we leave for future work.

Acknowledgement

We are grateful to the Gordon and Betty Moore Foundation for funding this research.

References

Adler, P.B., Seabloom, E.W., Borer, E.T., Hillebrand, H., Hautier, Y., Hector, A., Harpole, W.S., O.ÅôHalloran, L.R., Grace, J.B., Anderson, T.M., Bakker, J.D., Biederman, L.A., Brown, C.S., Buckley, Y.M., Calabrese, L.B., Chu, C.-J., Cleland, E.E., Collins, S.L., Cottingham, K.L., Crawley, M.J., Damschen, E.I., Davies, K.F., DeCrappeo, N.M., Fay, P.A., Firn, J., Frater, P., Gasarch, E.I., Gruner, D.S., Hagenah, N., Hille Ris Lambers, J., Humphries, H., Jin, V.L., Kay, A.D., Kirkman, K.P., Klein, J.A., Knops, J.M.H., La Pierre, K.J., Lambrinos, J.G., Li, W., MacDougall, A.S., McCulley, R.L., Melbourne, B.A., Mitchell, C.E., Moore, J.L., Morgan, J.W., Mortensen, B., Orrock, J.L., Prober, S.M., Pyke, D.A., Risch, A.C., Schuetz, M., Smith, M.D., Stevens, C.J., Sullivan, L.L., Wang, G., Wragg, P.D., Wright, J.P., Yang, L.H., 2011. Productivity is a poor predictor of plant species richness. Science 333, 1750–1753.

Agard, J.B.R., Hubbard, R.H., Griffith, J.K., 1996. The relation between productivity, disturbance and the biodiversity of Caribbean phytoplankton: Applicability of Huston's dynamic equilibrium model. Journal of Experimental Marine Biology and Ecology 202, 1L 17.

Agawin, N.S.R., Duarte, C.M., Agusti, S., 2000. Nutrient and temperature control of the contribution of picoplankton to phytoplankton biomass and production. Limnology and Oceanography 45, 591L 600.

Armstrong, R.A., McGehee, R., 1980. Competitive-exclusion. The American Naturalist 115, 151L 170.

Auad, G., Miller, A., Di Lorenzo, E., 2006. Long-term forecast of oceanic conditions off California and their biological implications. Journal of Geophysical Research 111, C09008.

Bakun, A., 1990. Global Climate Change and Intensification of Coastal Ocean Upwelling. Science 247, 198L 201.

Balech, E., 1960. The changes in the phytoplankton population off the California coast. In: The Changing Pacific Ocean in 1957 and 1958. California Cooperative Oceanic Fisheries Investigations Reports, 7:127–132.

Barton, A.D., Dutkiewicz, S., Flierl, G., Bragg, J., Follows, M.J., 2010. Patterns of diversity in marine phytoplankton. Science 327, 1509L 1511.

Bolin, R.L., Abbott, D.P., 1963. Studies on the marine climate and phytoplankton of the Central Coastal area of California, 1954-1960. California Cooperative Oceanic Fisheries Investigations Reports 9, 23L 45.
Bourrelly, P. (Ed.), 1985. Les algues d'eau douce. Initiation a la systematique (2eme edition revue et corrigee). Boubee, Paris.
Broquet, G., Edwards, C.A., Moore, A.M., Powell, B.S., Veneziani, M., Doyle, J.D., 2009. Application of 4D-Variational data assimilation to the California Current System. Dynamics of Atmospheres and Oceans 48, 69L 92.
Broquet, G., Moore, A.M., Arango, H.G., Edwards, C.A., 2010. Corrections to ocean surface forcing in the California Current System using 4D variational data assimilation. Ocean Modelling 36, 116L 132.
Bruland, K.W., Rue, E.L., Smith, G.J., 2001. Iron and macronutrients in California coastal upwelling regimes: Implications for diatom blooms. Limnology and Oceanography 46, 1661L 1674.
Cermeno, P., Maranon, E., Harbour, D., Figueiras, F.G., Crespo, B.G., Huete-Ortega, M., Varela, M., Harris, R.P., 2008. Resource levels, allometric scaling of population abundance, and marine phytoplankton diversity. Limnology and Oceanography 53, 312L 318.
Chavez, F.P., Barber, R.T., Kosro, P.M., Huyer, A., Ramp, S.R., Stanton, T.P., Demendiola, B.R., 1991. Horizontal transport and the distribution of nutrients in the coastal transition zone off Northern California – effects on primary production, phytoplankton biomass and species composition. Journal of Geophysical Research Oceans 96, 14833–14848.
Chesson, P., 2000. Mechanisms of maintenance of species diversity. Annual Review of Ecology and Systematics 31, 343–366.
Cloern, J.E., Dufford, R., 2005. Phytoplankton community ecology: principles applied in San Francisco Bay. Marine Ecology Progress Series 285, 11–28.
Di Lorenzo, E., Miller, A.J., Schneider, N. and McWilliams, J.C., 2005. The warming of the California Current system: Dynamics and ecosystem implications. American Meteorological Society, Boston, MA, ETATS-UNIS, 27 p.
Duarte, P., Macedo, M.F., da Fonseca, L.C., 2006. The relationship between phytoplankton diversity and community function in a coastal lagoon. Hydrobiologia 555, 3–18.
Edwards, M., Richardson, A.J., 2004. Impact of climate change on marine pelagic phenology and trophic mismatch. Nature 430, 881–884.
Fasham, M.J.R., Ducklow, H.W., Mckelvie, S.M., 1990. A nitrogen-based model of plankton dynamics in the ocean mixed layer. Journal of Marine Research 48, 591–639.
Fennel, K., Wilkin, J., 2009. Quantifying biological carbon export for the northwest North Atlantic continental shelves. Geophysical Research Letters L18605, http://dx.doi.org/10.1029/2009GL039818.
Follows, M.J., Dutkiewicz, S., Grant, S., Chisholm, S.W., 2007. Emergent biogeography of microbial communities in a model ocean. Science 315, 1843–1846.
Franks, P.J.S., Wroblewski, J.S., Flierl, G., 1986. Behavior of a simple plankton model with food-level acclimation by herbivores. Marine Biology 91, 121–129.
Goebel, N.L., Edwards, C.A., Zehr, J.P., Follows, M.J., 2010. An emergent community ecosystem model applied to the California Current System. Journal of Marine Systems 83, 221–241.
Grime, J.P., 1973. Competitive exclusion in herbaceous vegetation. Nature 242, 344–347.
Grover, J.P., Chrzanowski, T.H., 2004. Limiting resources, disturbance, and diversity in phytoplankton communities. Ecological Monographs 74, 533–551.
Gruber, N., Frenzel, H., Doney, S.C., Marchesiello, P., McWilliams, J.C., Moisan, J.R., Oram, J.J., Plattner, G.K., Stolzenbach, K.D., 2006. Eddy-resolving simulation of plankton ecosystem dynamics in the California Current System. Deep-Sea Research Part I-Oceanographic Research Papers 53, 1483–1516.
Hardin, G., 1960. Competitive exclusion principle. Science 131, 1292–1297.
Hodur, R.M., 1997. The Naval Research Laboratory's coupled ocean/atmosphere mesoscale prediction system (COAMPS). Monthly Weather Review 125, 1414–1430.
Huston, M., 1979. General hypothesis of species-diversity. The American Naturalist 113, 81–101.
Huston, M.A., 1999. Local processes and regional patterns: appropriate scales for understanding variation in the diversity of plants and animals. Oikos 86, 393–401.
Huston, M.A., Deangelis, D.L., 1994. Competitiion and coexistence – the effects of resource transport and supply rates. The American Naturalist 144, 954–977.
Hutchinson, G.E., 1961. The paradox of the plankton. The American Naturalist 95, 137–145.
Irigoien, X., Huisman, J., Harris, R.P., 2004. Global biodiversity patterns of marine phytoplankton and zooplankton. Nature 429, 863–867.
King, J.R., Agostini, V.N., Harvey, C.J., McFarlane, G.A., Foreman, M.G.G., Overland, J.E., Di Lorenzo, E., Bond, N.A., Aydin, K.Y., 2011. Climate forcing and the California Current ecosystem. ICES Journal of Marine Science 68, 1199–1216.
Kishi, M.J., Kashiwai, M., Ware, D.M., Megrey, B.A., Eslinger, D.L., Werner, F.E., Noguchi-Aita, M., Azumaya, T., Fujii, M., Hashimoto, S., Huang, D.J., Iizumi, H., Ishida, Y., Kang, S., Kantakov, G.A., Kim, H.C., Komatsu, K., Navrotsky, V.V., Smith, S.L., Tadokoro, K., Tsuda, A., Yamamura, O., Yamanaka, Y., Yokouchi, K., Yoshie, N., Zhang, J., Zuenko, Y.I., Zvalinsky, V.I., 2007. NEMURO - a lower trophic level model for the North Pacific marine ecosystem. Ecological Modelling 202, 12–25.
Legendre, P., Legendre, L., 1998. Numerical Ecology. Elsevier, New York.
Li, W.K.W., 2002. Macroecological patterns of phytoplankton in the northwestern North Atlantic Ocean. Nature 419, 154–157.
Longhurst, A., Sathyendranath, S., Platt, T., Caverhill, C., 1995. An estimate of global primary production in the ocean from satellite radiometer data. Journal of Plankton Research 17, 1245–1271.
McGowan, J.A., Bograd, S.J., Lynn, R.J., Miller, A.J., 2003. The biological response to the 1977 regime shift in the California Current. Deep-Sea Research Part II: Topical Studies in Oceanography 50, 2567–2582.
Mittelbach, G.G., Steiner, C.F., Scheiner, S.M., Gross, K.L., Reynolds, H.L., Waide, R.B., Willig, M.R., Dodson, S.I., Gough, L., 2001. What is the observed relationship between species richness and productivity? Ecology 82, 2381–2396.
Moore, J.K., Doney, S.C., Kleypas, J.A., Glover, D.M., Fung, I.Y., 2002. An intermediate complexity marine ecosystem model for the global domain. Deep-Sea Research Part II-Topical Studies in Oceanography 49, 403–462.
Omta, A.W., Llido, J., Garcon, V., Kooijman, S.A.L.M., Dijkstra, H.A., 2009. The interpretation of satellite chlorophyll observations: the case of the Mozambique Channel. Deep-Sea Research I 56, 974–988.
Partel, M., Zobel, M., 2007. Dispersal limitation may result in the unimodal productivity-diversity relationship: a new explanation for a general pattern. Journal of Ecology 95, 90–94.
Passarge, J., Hol, S., Escher, M., Huisman, J., 2006. Competition for nutrients and light: Stable coexistence, alternative stable states, or competitive exclusion? Ecological Monographs 76, 57–72.
Powell, T.M., Lewis, C.V.W., Curchitser, E.N., Haidvogel, D.B., Hermann, A.J., Dobbins, E.L., 2006. Results from a three-dimensional, nested biological-physical model of the California Current System and comparisons with statistics from satellite imagery. Journal of Geophysical Research Oceans 111, C07018.
Previdi, M., Fennel, K., Wilkin, J., Haidvogel, D., 2009. Interannual variability in atmospheric CO(2) uptake on the northeast US continental shelf. Journal of Geophysical Research 114, G04003, http://dx.doi.org/10.1029/2008JG000881.
Rosenzweig, M.L., Abramsky, Z., 1993. How are diversity and productivity related? In: Ricklefs, R.E., Schluter, L. (Eds.), Species Diversity in Ecological Communities: Historical and Geographical Perspectives. University of Chicago, Press, Chicago, Illinois, USA, pp. 52–65.
Shchepetkin, A.F., McWilliams, J.C., 2005. The regional oceanic modeling system (ROMS): a split-explicit, free-surface, topography-following-coordinate oceanic model. Ocean Modelling 9, 347–404.
Sommer, U., 1985. Comparison between steady-state and non-steady state competition – experiements with natural phytoplankton. Limnology and Oceanography 30, 335–346.
Sournia, A., Chrdtiennot-Dinet, M.-J., Ricard, M., 1991. Marine phytoplankton: how many species in the world ocean? Journal of Plankton Research 13, 1093–1099.
Spatharis, S., Mouillot, D., Danielidis, D.B., Karydis, M., Chi, T.D., Tsirtsis, G., 2008. Influence of terrestrial runoff on phytoplankton species richness-biomass relationships: A double stress hypothesis. Journal of Experimental Marine Biology and Ecology 362, 55–62.
Spatharis, S., Roelke, D.L., Dimitrakopoulos, P.G., Kokkoris, G.D., 2010. Analyzing the (mis)behavior of Shannon index in eutrophication studies using field and simulated phytoplankton assemblages. Ecological indicators 11, 697–703.
Veneziani, M., Edwards, C.A., Doyle, J.D., Foley, D., 2009a. A central California coastal ocean modeling study: 1. Forward model and the influence of realistic versus climatological forcing. Journal of Geophysical Research Oceans, 114.
Veneziani, M., Edwards, C.A., Moore, A.M., 2009b. A central California coastal ocean modeling study: 2. Adjoint sensitivities to local and remote forcing mechanisms. Journal of Geophysical Research Oceans, 114.
Venrick, E.L., 2009. Floral patterns in the California Current: The coastal-offshore boundary zone. Journal of Marine Research 67, 89–111.
Waide, R.B., Willig, M.R., Steiner, C.F., Mittelbach, G., Gough, L., Dodson, S.I., Juday, G.P., Parmenter, R., 1999. The relationship between productivity and species richness. Annual Review of Ecology and Systematics 30, 257–300.
Witman, J.D., Cusson, M., Archambault, P., Pershing, A.J., Mieszkowska, N., 2008. The relation between productivity and species diversity in temperate-arctic marine ecosystems. Ecology 89, S66–S80.
Wunsch, C., Heimbach, P., Ponte, R.M., Fukumori, I., Members, E.-G.C., 2009. The global general circulation of the ocean estimated by the ECCO-consortium. Oceanography 22, 88–103.

Please cite this article in press as: Goebel, N.L., et al., Modeled phytoplankton diversity and productivity in the California Current System. Ecol. Model. (2012), http://dx.doi.org/10.1016/j.ecolmodel.2012.11.008